Journal of Chromatography, 264 (1983) 393–404
Elsevier Science Publishers B.V., Amsterdam — Printed in The Netherlands

CHROM. 15,855

IMPROVED RADIOACTIVITY DETECTOR FOR FUSED-SILICA CAPILLARY COLUMNS*

PEDRO A. RODRIGUEZ*, CYNTHIA R. CULBERTSON and CYNTHIA L. EDDY
The Procter & Gamble Company, Miami Valley Laboratories, PO Box 39175, Cincinnati, OH 45247 (U.S.A.)
(Received February 23rd, 1983)

SUMMARY

^{14}C-labeled and unlabeled organic compounds eluting from fused-silica capillary columns were detected by the parallel combination of a radioactivity detector (RAD) and a flame ionization detector (FID). The RAD consists of a small-volume counter tube and ancillary electronics. It is constructed from readily available parts. For maximum signal-to-noise ratio, the RAD is operated at 70% counting efficiency. The resulting background is less than 5 cpm. The instrumentation delivers high chromatographic efficiency and eliminates combustion artifacts. Radioactive peaks are 12 sec wide, while the detection limit is *ca.* 440 cpm (0.2 nCi) for peaks with $k' \leqslant 5$. No degradation in column performance is apparent in the FID trace.

INTRODUCTION

Separations of ^{3}H- and ^{14}C-labeled materials by gas chromatography (GC), and their detection in the gas stream, are well documented in the literature. An excellent review of this topic appeared in this journal[1]. The continuous monitoring of ^{14}C-labeled and unlabeled compounds is typically performed after splitting the eluted sample. One fraction of the sample goes to a flame ionization detector (FID) while the remaining fraction is counted. Frequently, the counting is done after conversion of the compounds to $^{14}CO_2$ (refs. 2–4). This conversion facilitates transfer of the radiolabel to the radioactivity detector (RAD) and permits room-temperature operations of the RAD. In addition, it eliminates possible compound-related quench problems.

The RAD can be a flow-through detector of a variety of types: the $^{14}CO_2$ can be trapped in a liquid stream which contains a scintillator, and then counted, or it can be trapped in aqueous NaOH and counted by flowing the liquid stream through a cell packed with a solid scintillator[5]. Alternatively, the $^{14}CO_2$ can be counted as a gas by means of a solid scintillator[6,7] or a proportional counter[2–4,8].

The use of flow-through detectors requires a compromise between sensitivity

* This paper was presented in part at the *International Symposium, Capillary Chromatography '82, Tarrytown, NY, October 4–6, 1982.*

and resolution. Sensitivity is dependent on the counting time, and therefore depends on the residence time of the material in the counter. A long residence time increases sensitivity but may impair resolution. For packed-column GC, a long residence time (*e.g.*, 60 sec) may not significantly affect resolution. This is not true for capillary columns where the peak-width may be only a few seconds.

Instrumentation to perform FID and RAD detection on effluents from capillary columns has been reported[6,8,9]. Gross *et al.*[6] used a microfurnace to convert the radiolabel to $^{14}CO_2$ to minimize band spreading prior to radioactivity detection. A commercial flow monitor, equipped with an anthracene cell (total volume *ca.* 7 ml), was used as the detector. The flow-rate through the detector was adjusted to 12–14 ml/min with a suction pump. They reported a limit of detection of 7 Bq (420 dpm or 0.2 nCi). We estimated the minimum peak-width of the radioactive peaks shown at *ca.* 30–60 sec.

Ernst *et al.*[8] adapted a commercial gas flow proportional counter (with a 20-ml volume) for use with capillary columns. Make-up gas was added to adjust the gas flow through the counter to 60 ml/min. They estimated their detection limit at about 100 dpm (0.05 nCi). However, based on their experimental conditions, the minimum peak-width of the radioactive peaks is likely to exceed 30 sec.

A short residence time in the flow-through RAD is necessary to match better the resolution available by the use of capillary columns. However, a short time requires a high signal-to-noise ratio to achieve an acceptable detection limit.

Gas flow-through proportional counters have the potential for higher signal-to-noise ratios than approaches based on the use of solid or liquid scintillators. For example, an anti-coincidence gas counter having *ca.* 95% efficiency for ^{14}C and a background of *ca.* 1 cpm has been reported[10]. In addition, the counter tube and ancillary instrumentation can be simple and reliable. For these reasons, a gas flow-through proportional counter was chosen for our design.

In this report we describe the instrumentation developed for parallel detection of carbon-containing and ^{14}C-labeled compounds separated by capillary GC. A small-volume counter, a simple and inexpensive electronics package and the elimination of combustion artifacts combine to produce low detection limits while maintaining the narrow bandwidths associated with capillary columns.

EXPERIMENTAL

Gas chromatograph

A Perkin-Elmer 3920 gas chromatograph, equipped with a quartz injector/trap[11], was modified to accept the RAD. A diagram of the instrumentation is shown in Fig. 1. Two modifications were performed: first, a splitter was installed in the detector manifold section of the gas chromatograph. Second, access to the splitter from the right side of the unit was provided by drilling a 1-in. hole through the side panel and a 0.5-in. hole through the manifold wall. A Vycor combustion tube was brought into the manifold through these holes. The larger hole holds an Inconel tube used to house the combustion tube.

The splitter and the inlet of the combustion tube are shown in Fig. 2. The necessary assemblies were made from stainless-steel (SS) Swagelok fittings: 1/2-in. to 1/16-in. reducing union and two 1/16-in. tees. The union and one of the tees were

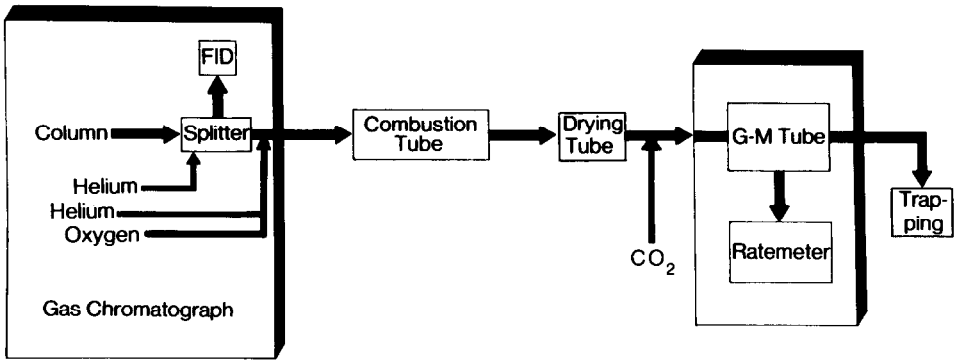

Fig. 1. Diagram of FID/RAD for detection of ^{14}C-labeled compounds. G-M = Geiger-Müller gas flow-through proportional counter.

drilled to accept 1/16-in. O.D. SS tubes which were silver-soldered in place.

These tubes are used to add make-up gases. The split ratio was adjusted by varying the length of 0.2-mm I.D. fused-silica lines connecting the modified tee to the detectors. Two 15-in. lengths were used to produce a *ca.* 50/50 split. Vespel ferrules were used to obtain gas-tight connections. A make-up gas (I, Fig. 2), He at 20 ml/min, was added to the modified tee to keep the residence time of a peak in the splitter to less than 0.1 sec.

Combustion tube

A 60-cm long Vycor tube (6 mm O.D., 4 mm I.D.) was loosely packed with a mixture of ground quartz and CuO wire (0.4–0.5 mm diameter): 6–8 g of mixture occupied a section of tube *ca.* 23 cm long. Quartz wool was used to keep the bed in

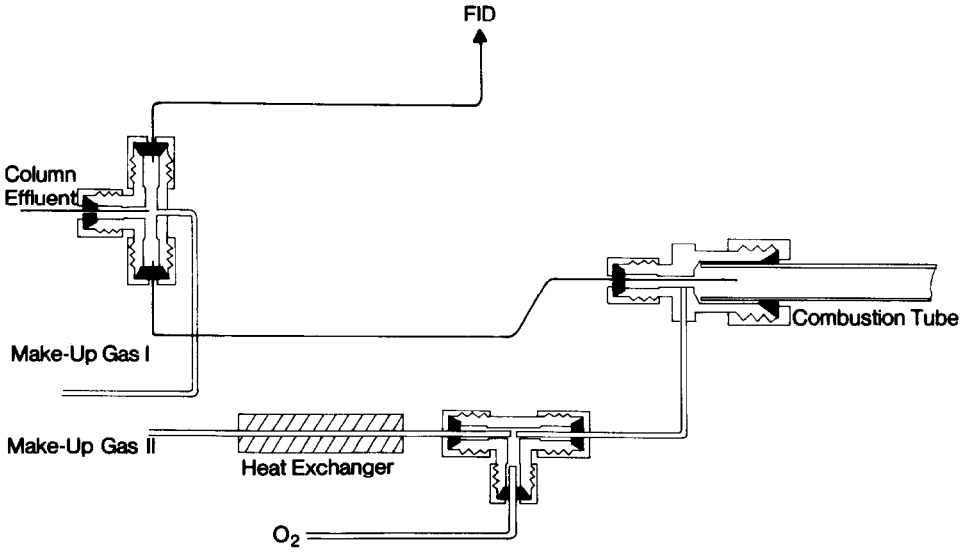

Fig. 2. Diagram of splitter and combustion tube inlet. All components shown are installed in the detector manifold of the gas chromatograph.

place and quartz rod inserts (3 mm O.D.) were used to occupy the empty ends of the tube.

The combustion tube was housed within a 45 × 2.5 cm O.D. Inconel tube and was placed inside a combustion furnace (Model 55035; Lindberg, Watertown, WI, U.S.A.) kept at 800°C. The placement of the assemblies is such that the head of the combustion bed is 10 cm from the end of the furnace nearest to the gas chromatograph. The furnace was located next to the wall of the gas chromatograph.

Make-up gas (II, Fig. 2), helium at 49 ml/min, was added to the combustion tube via the modified reducing union. A trickle of oxygen, at *ca.* 1 ml/min, was added to the second make-up gas via the tee placed in the detector manifold. The effluent of the combustion tube was passed through a drying tube containing $Mg(ClO_4)_2$, and was mixed with quench gas (CO_2, 6 ml/min) prior to entering the counter tube.

Split ratio measurements

The FID jet tip was removed and replaced with a SS tube silver-soldered to the base of a FID jet. The split ratio was calculated from either measured flow-rates or from radioactivity collected at the FID and RAD. The $^{14}CO_2$ was collected with an ethanolamine-based cocktail. Liquid scintillation counting (LSC) was done by a Packard Tri-Carb Scintillation spectrometer (Model 2001; Packard, Downers Grove, IL, U.S.A.). The cocktail collection efficiency for CO_2 and intact organic compounds was 100%, while the combined scintillation/counting efficiency of the cocktail and counter was 59%.

Some split ratio measurements, and all of the experiments designed to quantitatively measure contamination, were performed without a column. In these experiments, transfers of materials from the injector/trap to the splitter were made via a 0.3 mm I.D. PTFE line.

Contamination measurements

For these experiments a 10-ml sample of $^{14}CH_2Br_2$ in air, containing *ca.* 150 μg and *ca.* 48 nCi, was trapped in the injector/trap. After transfer to the detectors via the PTFE line, the radioactivity was collected for 5 min. The split ratio was calculated from these data. Residual radioactivity was calculated from the radioactivity collected for an additional 5 min.

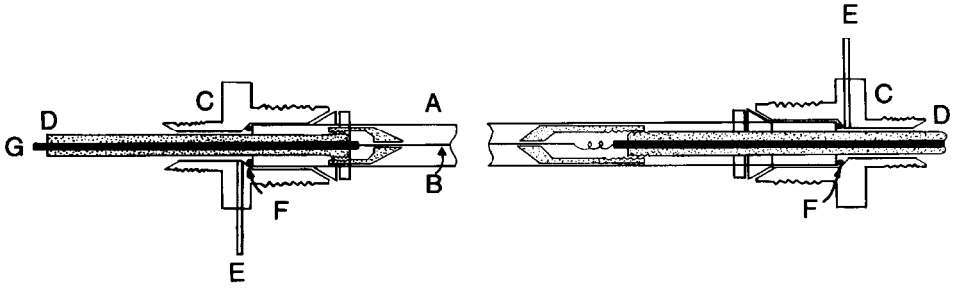

Fig. 3. Diagram of counter tube. A = 12.5-mm O.D. SS tube; B = tungsten wire; C = nylon reducing union; D = Delrin holders; E = 1/16-in. O.D. SS tube; F = O-ring spacer; G = brass rod.

Radioactivity detector (RAD)

The RAD consists of a counter tube and associated electronics. The counter tube is a 10 cm × 12.5 mm O.D. × 11 mm I.D. SS tube. The interior was polished to a smooth finish. The tube was polarized with a −2.2 kV regulated supply (No. 224; Keithley, Cleveland, OH, U.S.A.). The anode is a 5 cm × 0.1 mm O.D. tungsten wire. The anode is centered in the tube by Delrin holders placed in modified Nylon 1/2-in. to 1/4-jn. reducing unions. These unions were drilled to accept a 1/16-in. O.D. tube. A tube was fixed to each of the unions with epoxy glue. A schematic diagram is shown in Fig. 3. The assembly is housed in a 1-in. thick lead shield.

Current pulses occurring at the anode are converted to a voltage by an operational amplifier (gain = $2 \cdot 10^{-8}$ A/V), stretched in time (time constant, τ = 0.5 msec), discriminated with respect to amplitude and time, and counted. The counter module (TIL 307; Texas Instruments, Dallas, TX, U.S.A.) serves also as a display and latch. The contents of the latches are updated every 6 sec and displayed on a recorder via a 12-bit digital-to-analogue converter. A diagram is shown in Fig. 4.

Calculations

The displayed counts (RAD counts) are related to the radioactivity injected by the equation

$$\text{RAD (counts)} = A \times S \times \varphi \times E \times (V/F)$$

where A = radioactivity injected (dpm), S = split ratio, φ = fraction of sample

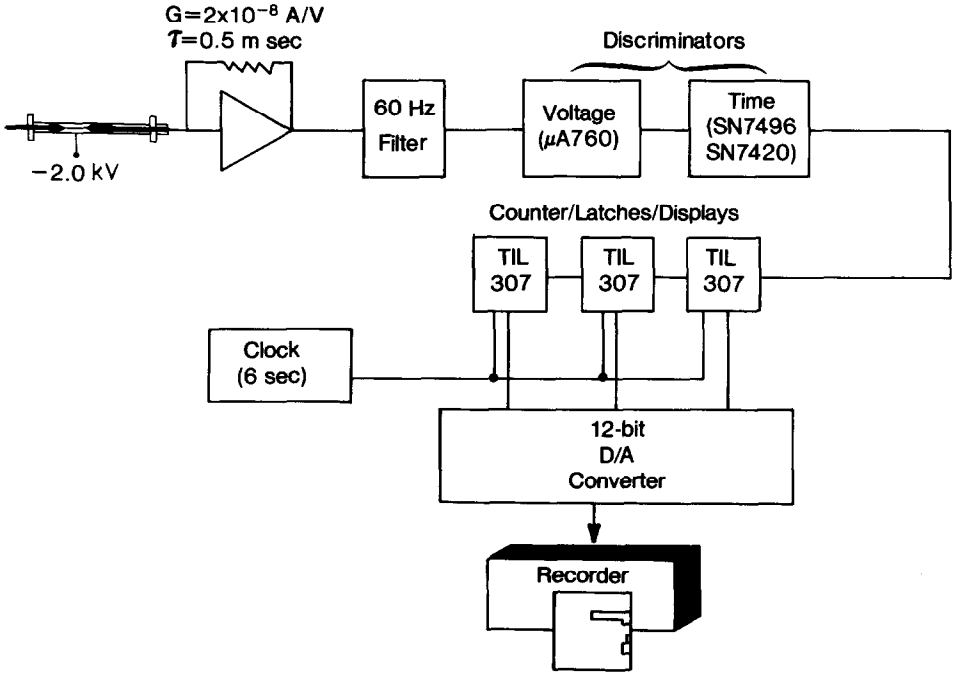

Fig. 4. Diagram of counter electronics. G = Gain; D/A = digital-to-analogue.

recovered from the system, E = counter efficiency and (V/F) = residence time in the counter (V is the effective counter volume in mL, F is the gas-flow rate in ml/min). For most of the work presented here, $S = 0.46$, $E = 0.70$ and $V/F = 0.070$ min. Under these conditions the equation reduces to:

$$\text{RAD (counts)} = A \times \varphi \times (0.023)$$

φ was calculated by dividing the radioactivity collected from the RAD effluent by the product of A, S and the cocktail trapping/counting efficiency.

Racioactive standards

n-Decane, *n*-$^{14}C_{10}$ (1-^{14}C, 7.5 mCi/mmol), and *n*-decanol, *n*-$^{14}C_{10}OH$ (1-^{14}C, 7.5 mCi/mmol), were purchased from ICN (Irvine, CA, U.S.A.). Naphthalene (1(4,5,8)-^{14}C, 5 mCi/mmol) was purchased from Amersham (Amersham, Great Britain). Working standards were prepared by dilution in pentane. Dibromo [^{14}C]methane was purchased from California Bionuclear Corp. (Sun Valley, CA, U.S.A.) and was diluted with the cold materialm to an activity of 0.054 mCi/mmol.

RESULTS AND DISCUSSION

Several experimental variables affect the split ratio. To eliminate column-oven temperature as a variable, the splitter was placed in the thermostated detector manifold of the gas chromatograph. However, the split is a sensitive function of the backpressure generated downstream from the splitter.

The effect of downstream pressure changes on the split ratio is minimized by reducing the backpressure generated by the components placed after the fused-silica lines: the FID, the combustion tube and the counter tube. Of these, only the combustion tube presents a problem. The other components generate less than 0.5 p.s.i. at the flow-rates used.

When the combustion tube was packed with CuO particles, 0.1–0.3 mm diameter, and in the absence of O_2, the backpressure exceeded 13 p.s.i. with the bed at 800°C. Dilution of the packing with ground quartz and the use of CuO wire, 0.3–0.5 mm long, produced a more porous bed with lower backpressure. A 3:1 mixture of CuO wire and quartz particles, 0.5–1 mm mean diameter, generated 3.4 p.s.i. of backpressure at 800°C. However, after three injections of $^{14}CH_2Br_2$, corresponding to the combustion of a total of *ca.* 210 μg of compound, the backpressure increased to 6.4 p.s.i. The split ratio (RAD/FID) changed from 57/43 to less than 50/50, as shown in Fig. 5I, curve C. Furthermore, the radioactivity remaining in the combustion tube, after the elution of the main body of radioactivity, increased with mass or number of injections made. This is shown in Fig. 5II, curve C.

The changes in backpressure and the residual radioactivity in the combustion tube are a consequence of the surface exhaustion of the CuO bed. As the surface changes, the Cu-containing particles fuse together, thereby decreasing the permeability of the packing and increasing the adsorptive capacity of the bed. Because of the high temperature, the adsorbed compounds eventually decompose or diffuse to oxygen-containing bed sites. The result is a slow release of radioactivity from the combustion tube. Practical consequences of this behavior are poor peak shape and

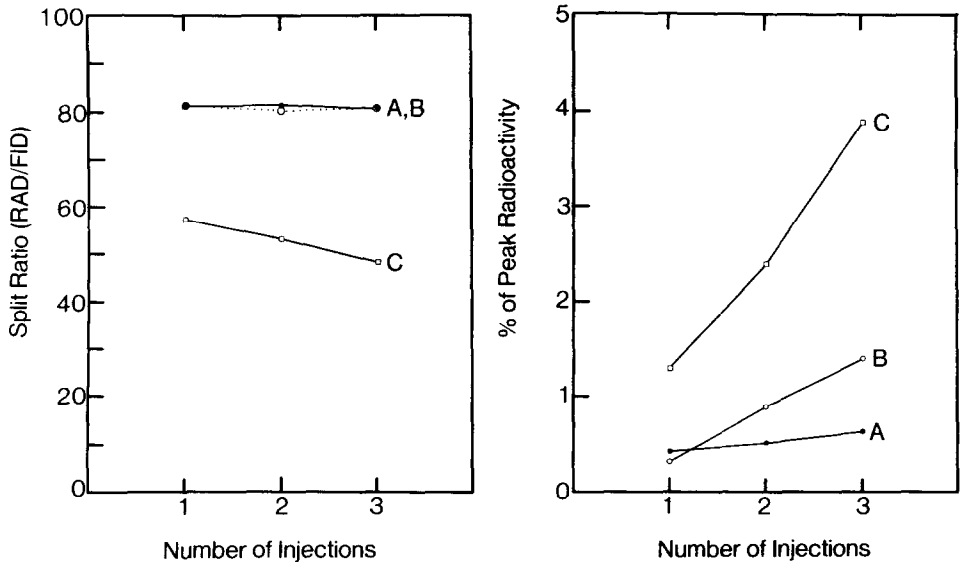

Fig. 5. I, Variation of split ratio after injection of $^{14}CH_2Br_2$; II, radioactivity remaining in the combustion tube after injection of $^{14}CH_2Br_2$. Bed composition: A, CuO: quartz mixture 5:1 (w/w) + a trickle of O_2; B, CuO: quartz mixture 5:1 (w/w) with no added O_2; C, CuO: quartz mixture 3:1 (w/w).

poor recovery of radioactivity. This is illustrated in Fig. 6, where only 61 % of the expected radioactivity is found under the peak. Note the increased background after the peak and the lack of corresponding changes in the FID trace. Increasing the CuO wire length increases bed permeability and decreases the retention of radioactivity in the combustion tube. A 80:20, RAD/FID ratio was selected to illustrate these two points. Curve B, Fig. 5I and II, corresponds to a 5:1 CuO: quartz bed packed with 1–3 mm CuO wire and 0.3–0.5 mm quartz particles. With this packing the backpressure is less than 2 p.s.i. and the split ratio remains constant (5I). The radioactivity remaining in the combustion tube is *ca.* 1.5% after three injections, as shown in Fig. 5II, curve B. Further decreases in residual radioactivity were achieved by the continuous introduction of a trickle of oxygen into the combustion tube, as shown in Fig. 5II, curve A.

While the introduction of O_2 into the combustion tube results in a stable bed that requires no repacking, it changes the operating parameters of the counter tube. This is apparent in Fig. 7. A broad efficiency maximum is observed in the absence of O_2 (7A) but a continuous increase in efficiency with polarizing voltage is seen when O_2 is present (7B).

The broad maximum, rather than the expected Geiger-Müller plateau, is a consequence of the d.c. approach, the gain and the time constant we have chosen to process the current pulses. As the internal gain of the tube increases with polarizing voltage, the magnitude of the current pulses also increases. These pulses are very large in the Geiger-Müller region, and, because of their magnitude, they produce short-term saturation of the amplifier at the chosen gain. The saturation and long time constant combine to produce pulse pile-up and an apparent decrease in efficiency.

Because O_2 is a more efficient quencher than CO_2, its use requires a higher tube voltage to achieve the same counting efficiency. However, there is no apparent

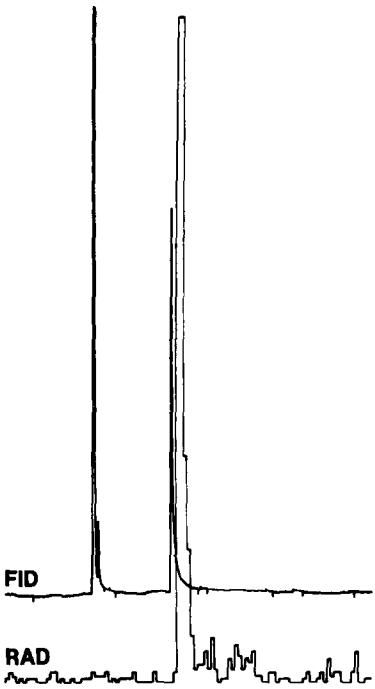

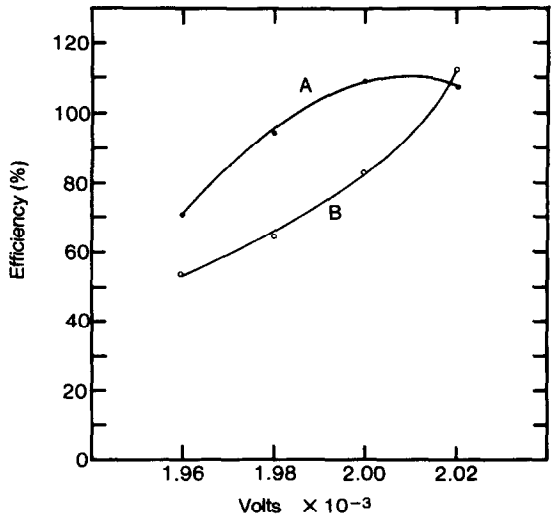

Fig. 6. Chromatogram of *n*-decanol. Combustion without added oxygen. Isothermal run: 140°C, SE-54, 30 m × 0.32 mm J&W fused-silica column. Mass (activity) injected = 96 ng (4.6 nCi). Injection volume = 5.8 µl. FID sensitivity = 5 pA full scale. Split: 80/20 (RAD/FID). Recovery of radiolabel under the peak: 61 %

Fig. 7. Counter-tube efficiency as a function of gas composition. A, He 59 ml/min, CO_2 6 ml/min; B. He 59 ml/min, CO_2 6 ml/min, O_2 1 ml/min.

Geiger-Müller region. This is inconsequential to the operation of the RAD because we operate the counter tube in the proportional region where efficiency is dependent on applied voltage. This mode of operation does not represent a serious drawback when highly regulated supplies (0.01 %) are used and when the current measurement approach (*i.e.*, a d.c. measurement with the anode at virtual ground) ensures a constant field gradient across the tube. Therefore, to operate the tube in the presence of O_2, it is only necessary to use a more negative potential to achieve the desired efficiency. For maximum signal-to-noise ratio, the tube is operated at 70 % efficiency. The resulting background is 3–5 cpm.

The chromatographic performance of the system is illustrated in Fig. 8. No increase in background radioactivity is seen after the elution of n-$^{14}C_{10}$. Because this compound elutes shortly after the solvent (capacity factor, $k' < 1$) the background radioactivity after the C_{10} peak would have shown an increase if there were surface exhaustion of the combustion bed by the solvent. Since the mass present in the solvent peak is likely to exceed that of any other compound in the chromatogram, we expect a constant, low radioactivity background under most separation conditions.

The number of theoretical plates, N, calculated from the FID trace of the n-C_{12} hydrocarbon (isothermal run, $k' \approx 3$), is *ca.* 10^5. For peaks with k' between 3

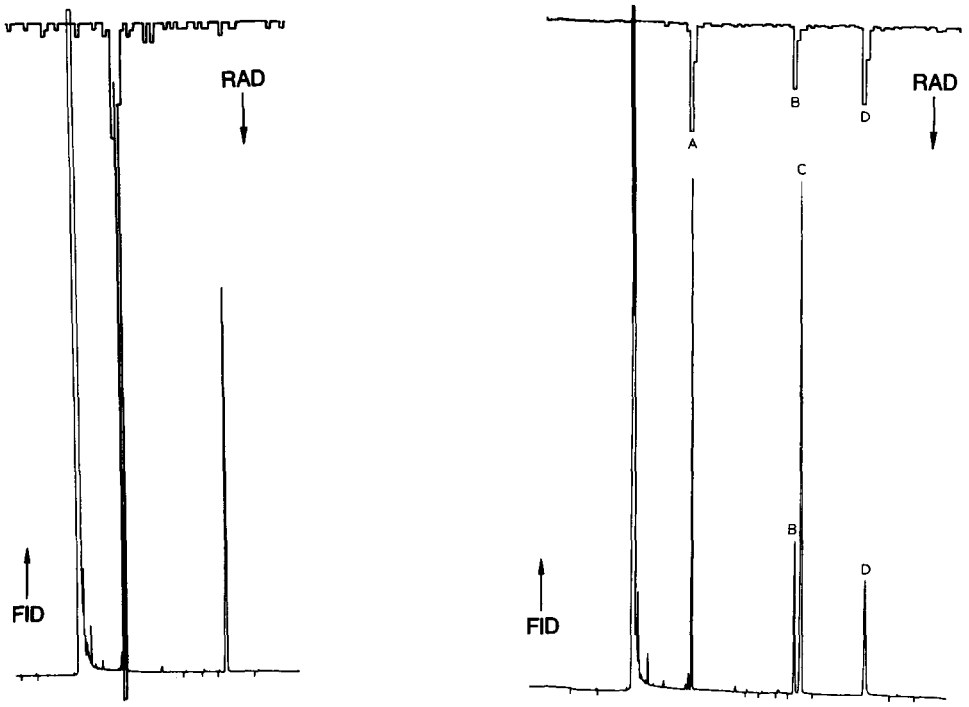

Fig. 8. Chromatogram of n-$^{14}C_{10}$ and n-C_{12} hydrocarbons in pentane. Temperature-programmed run: 110°C isothermal hold 4 min, 4°C/min to 120°C and hold. Durabond 5 J&W, 30 m × 0.32 mm I.D. Absolute recovery of radiolabel under the peak: 80%. RAD efficiency: 68%. Sensitivity: 100 counts full scale. RAD/FID split ratio: 46/54. Mass injected: *ca.* 70 ng per compound.

Fig. 9. Chromatogram of ^{14}C-labeled standard materials and cold n-C_{12}. Mass (radioactivity) injected: A, n-$^{14}C_{10}$, 63 ng (2.4 nCi); B, ^{14}C-Naphthalene, 25 ng (0.9 nCi); C, n-C_{12}, 110 ng; D, n-$^{14}C_{10}OH$, 38 ng (1.5 nCi).

TABLE I

ANALYSIS OF RADIOLABELED STANDARDS

Mass (radioactivity) injected: n-$^{14}C_{10}$, 50–80 ng (2.6–4.2 nCi); ^{14}C-naphthalene, 20–30 ng (0.8–1.2 nCi); n-$^{14}C_{10}OH$, 30–50 ng (1.4–2.4 nCi).

	Nominal distribution (%)		*Experimental distribution (%)*		
	Radioactivity	*Mass*	*FID area*	*$^{14}CO_2$ liquid scintillation*	*RAD counts*
n-$^{14}C_{10}$	54	50	52 ± 1	50 ± 1	47 ± 2
Naphthalene	14	20	21 ± 1	18 ± 1	19 ± 5
n-$^{14}C_{10}OH$	30	30	27 ± 1	32 ± 1	35 ± 3

TABLE II

FID RESPONSE FACTOR DETERMINATION BY "COLD" AND RADIOLABELED STANDARDS

No. of measurements	*Mass (ng) range tested*	*Compound*	*Apparent response factor (Coul/g compound)*	*Absolute recovery (%)*	*Corrected response factor (Coul/g compound)*
5	36–90	n-C_{12}	0.014 ± 0.001		0.018
6	38–94	n-$^{14}C_{10}$	0.014 ± 0.001	80 ± 4	0.018

and 5, the chromatographic efficiency calculated from the RAD trace is *ca.* $2 \cdot 10^4$ theoretical plates.

While the high chromatographic efficiency measured with hydrocarbons is an indicator of splitter performance, a more severe test is posed by the quantitative, temperature-programmed analysis of a mixture containing polar compounds. A chromatogram is shown in Fig. 9. The results are summarized in Table I.

The distribution of radioactivity recovered as $^{14}CO_2$ from the RAD agrees, withinin experimental error, with the distribution calculated from the RAD counts. The larger relative error observed in the RAD distribution is the result of the

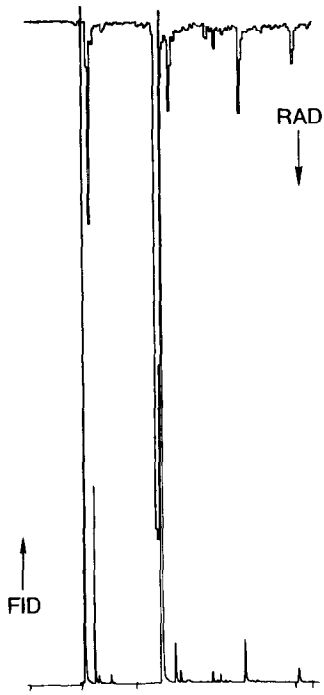

Fig. 10. Chromatogram of underivatized ^{14}C-diethylenetriamine. Conditions: 140°C isothermal hold 2 min, 8°C/min to 190°C and hold. Carbowax J&W, specially deactivated for amines, 30 m × 0.25 mm I.D. RAD/FID split: 46/54. RAD sensitivity = 1000 counts full scale. Mass (radioactivity) injected = 2 μg (500 nCi).

TABLE III

RADIOCHEMICAL DATA OF DIETHYLENETRIAMINE (DETA) SAMPLE

Specfic activity determination	
FID area	$(5.77 \pm 0.08) \cdot 10^6$
Mass DETA eluted (g)*	$1.15 \cdot 10^{-6}$
$^{14}CO_2$ activity (cpm)	$(1.68 \pm 0.1) \cdot 10^5$
Radioactivity eluted (nCi)**	280
Calculated DETA specific activity (mCi/mmol)	25
Bulk specific activity reported (mCi/mmol)	20

Distribution and radiopurity of DETA sample by three detection methods

	FID (area %)	*LSC (cpm %)*	*RAD (counts %)*
Ethylenediamine	7.1 ± 0.3	6.3 ± 0.4	7.3 ± 1.1
DETA	85.5 ± 0.1	82.7 ± 1.9	82.6 ± 2.3
Unknown I	2.4 ± 0.3	4.3 ± 1.5	3.8 ± 0.4
II	3.4 ± 0.2	4.4 ± 0.5	3.5 ± 1.2
III	1.6 ± 0.1	2.4 ± 0.7	2.8 ± 0.6

* Calculated from sensitivity of FID in C/g carbon, carbon content of DETA and split ratio.
** Calculated from scintillation/counting efficiency and split ratio.

short residence time and low activity of the samples. Less than 50 RAD counts were recorded for the naphthalene peak.

The distribution calculated from FID areas agrees with the nominal mass distribution calculated from the radioactivity and the specific activity of the standards. This agreement is due to the similar FID response factors and transfer efficiency (recovery) of the compounds studied.

Knowledge of the transfer efficiency of a compound is most important when performing parts-per-billion ($1/10^9$) analyses on gaseous samples. This is true because it is nearly impossible to prepare accurate gaseous standards at those levels and the internal-standard technique is not generally applicable. The use of a radiolabeled model compound, if not the analyte itself, allows accurate calibration of the FID detector. Once this is done, the FID is available to perform ultra-trace analyses. An illustration of this application is shown in Table II, where the apparent FID response measured by injecting known masses of n-$^{14}C_{10}$ is corrected by the transfer efficiency of the compound. As expected, the uncorrected values measured for the n-C_{10} and n-C_{12} hydrocarbons agree since they should have the same transfer efficiency. However, only 80% of the compound is reaching the detectors. Therefore, for accuracy, the results can now be corrected to account for the transfer efficiency of the system.

Finally, the ability to perform accurate mass and radioactivity measurements can be used in establishing radiopurity and specific activity. This point and the high resolution possible with the equipment are illustrated in Fig. 10 and Table III.

ACKNOWLEDGEMENTS

Our thanks to R. J. Lloyd for helpful suggestions and discussions.

REFERENCES

1 M. Matucha and E. Šmolková, *J. Chromatogr.*, 127 (1976) 163.
2 D. K. Albert, R. L. Stoffer and R. D. Kaplan, *J. Chromatogr. Sci.*, 12 (1974) 183.
3 A. V. Barooshian, M. J. Lautenschieger and W. G. Harris, *Anal. Biochem.*, 44 (1971) 543.
4 O. Helmich and J. Hradec, *J. Chromatogr.*, 91 (1974) 505.
5 A. Karmen and N. S. Longo, *J. Chromatogr.*, 112 (1975) 637.
6 D. Gross, H. Gutekunst, A. Blaser and H. Hamböck, *J. Chromatogr.*, 198 (1980) 389.
7 A. Karmen, I. McCaffrey and R. L. Bowman, *J. Lipid Res.*, 3 (1962) 372.
8 L. A. Ernst, G. T. Emmons, J. D. Naworal and I. M. Campbell, *Anal. Chem.*, 53 (1981) 1959.
9 H. Weber, M. Höller and H. Breuer, *J. Chromatogr.*, 235 (1982) 523.
10 T. H. Simpson, *J. Chromatogr.*, 38 (1968) 24.
11 P. A. Rodriguez, C. L. Eddy, G. M. Ridder and C. R. Culbertson, *J. Chromatogr.*, 236 (1982) 39.